Apoptin causes apoptosis in HepG-2 cells via Ca2+ imbalance- triggered mitochondrial apoptotic pathway

Xiaoyang Yu
Changchun University of Chinese Medicine
Tongxing Wang
Chinese Academy of Agricultural Sciences
Yue Li
Changchun University of Chinese Medicine
Yiquan Li
Changchun University of Chinese Medicine
Bing Bai
Changchun University of Chinese Medicine
Jinbo Fang
Changchun University of Chinese Medicine
Jicheng Han
Changchun University of Chinese Medicine
Shanzhi Li
Changchun University of Chinese Medicine
Zhiru Xiu
Changchun University of Chinese Medicine
Zirui Liu
Chinese Academy of Agricultural Sciences
Xia Yang
Changchun University of Chinese Medicine
Yaru Li
Changchun University of Chinese Medicine
Guangze Zhu
Changchun University of Chinese Medicine
Ningyi Jin
Changchun University of Chinese Medicine
Chao Shang
Chinese Academy of Agricultural Sciences
Xiao Li

Chinese Academy of Agricultural Sciences
Yilong Zhu (zhuyilong66@163.com)
Changchun University of Chinese Medicine

Research Article

Keywords: Apoptin, endoplasmic reticulum stress, Ca2+ imbalance, mitochondria structural injury, mitochondria apoptosis pathway

Posted Date: May 13th, 2022

DOI: https://doi.org/10.21203/rs.3.rs-1619281/v1

Abstract

Apoptin is derived from the chicken anemia virus and exhibits specific cytotoxic effects against tumor cells. Herein, we found that Apoptin induced a strong and lasting endoplasmic reticulum (ER) stress response and Ca^{2+} imbalance, and triggered the mitochondrial apoptotic pathway. The aim of this study was to explore the mechanisms by which Apoptin exhibited anti-tumor effects on the HepG-2 cells. The intracellular level of calcium (Ca^{2+}) was induced by ER stress and determined by electron microscopy, flow cytometry and fluorescence staining. Mitochondrial injury was determined by mitochondrial membrane potential, electron microscopy. Western blotting was used to investigate the levels of key proteins in the ER stress and the apoptotic pathway in the mitochondria. The relationship between Ca^{2+} level and apoptosis on Apoptin-treating cells was analyzed using Ca^{2+} chelator (BAPTA-AM), flow cytometry and fluorescence staining. We also investigated the *in vivo* effects of Ca^{2+} imbalance on the mitochondrial apoptotic pathway using the tumor tissues xenografted on nude mice. *In vitro* and *in vivo* experiments showed that Apoptin caused an imbalance in Ca^{2+}, and increased the expression levels of Smac/Diablo and Cyto-C. In summary, Apoptin induced apoptosis in HepG-2 cells via Ca^{2+} imbalance-triggered mitochondrial apoptotic pathway. This study provided a new direction for antitumor research in Apoptin.

1 Introduction

Apoptin (GenBank: AY171617.1) is derived from chicken anemia virus, which exhibits cytotoxicity that is specific to tumor cells [12, 20]. In most of the cell lines investigated thus far, Apoptin has been shown to induce apoptosis in tumor cells via the intrinsic mitochondrial pathway. Apoptin reduces the mitochondrial membrane potential in tumor cells and induces the mitochondria to release cytochrome c (Cyto-C) and apoptosis inducing factor (AIF) [1, 11, 19], thus resulting in apoptosis. Apoptin-induced apoptosis is known to occur independently of p53 [35]. In our research, we found that Apoptin induced a strong and long-lasting endoplasmic reticulum stress. However, as yet, the specific mechanism that underlying the association between ER stress and Apoptin has yet to be elucidated.

The endoplasmic reticulum (ER) is an important intracellular organelle and participates in a number of cellular processes *in vivo*. The ER is also the main site of calcium (Ca^{2+}) storage. Ca^{2+} can be stored in the ER in concentrations of 10–100 mmol/L, but is present at concentrations of 100–300 nmol/L in the cytoplasm. A strong and lasting ER stress response creates an imbalance in Ca^{2+}. ER stress is known to involve the Endoplasmic Reticulum Kinase (PERK) pathway [9, 15, 17], the Inositol-Requiring Enzyme1 (IRE1) pathway [7, 24, 30], and the Activating Transcription Factor 6 (ATF-6) pathway [31, 32].

As the key site of energy transformation, the mitochondria also represent the main regulatory site for apoptosis and also play a key role in most of the regulatory processes related to apoptosis. An abnormal change in the mitochondrial membrane potential triggers the release of apoptosis-related proteins from the mitochondria, including AIF, High-Temperature Requirement Protein A2 (HtrA2), Endonuclease G (Endo

G), Apoptosis-Related Proteins (ARTs), Second Mitochondria-Derived Activator of Caspase/Direct IAP Binding Protein with Low pl (Smac/Diablo), and Cyto-C. Ca^{2+} imbalance caused by ER stress can affect the structure and function of the mitochondria. Despite that some research has indicated that Apoptin induces mitochondria to release Cyto-C and AIF, no previous study has investigated how Apoptin-induced ER stress caused Ca^{2+} imbalance and influenced the structure and function of the mitochondria. Moreover, previous studies have not investigated the specific effect of Apoptin on the expression of key apoptosis-related proteins in the mitochondria, such as HtrA2, Smac/Diablo, Endo G, and ATRS.

Therefore, it is of great significance to investigate the specific effect of ER stress on the ER and apoptosis-related pathways in the mitochondria with regards to the induction of apoptosis. In the present study, we demonstrated that Apoptin can induce ER stress, cause Ca^{2+} imbalance, affect the structure and function of the mitochondria, and induce significant changes in the expression of key proteins related to the ER stress and the mitochondria. Our research involved the assessment of dynamic changes in the ER and mitochondria, the determination of Ca^{2+} levels, the Western blotting and immunohistochemical analysis of tumor tissue from a tumor-bearing nude mouse model.

2 Materials And Methods

2.1 Materials

Human hepatoma cell line HepG-2 was purchased from the Cell Bank of the Chinese Academy of Sciences (Shanghai, China). We also used a recombinant type 5 adenovirus (Ad-Apoptin; hereafter referred to as Ad-Vp3) that contained a CMV promoter and the Apoptin gene from chicken anemia virus. We used the recombinant type 5 adenovirus (hereafter referred to as Ad-Mock) without the Apoptin gene as a blank control. Ad-Vp3 and Ad-Mock were constructed previously in our laboratory.

Six-week-old male BALB/c nude mice were housed in light, comfortable temperature and humidity room (22 ± 2°C, 50 ± 5% relative humidity), given solid diet (Changchun billion Adams Laboratory Animal Technology Co., Ltd.) and sterilized tap water. All mice were obtained from Beijing vital River Laboratory Animal Technology Co., Ltd., and the animal experiment protocols were approved by the Institutional Animal Care and Use Committee (IACUC) of the Changchun University of Chinese Medicine. All mice surgery was performed under 40 mg/kg 1% sodium pentobarbital via intraperitoneal injection.

Dihydrorhodamine 123 (DHR) (No. D632), JC-1 (No. T3168), MitoTracker™ Red CMXRos (TMRM) (No. M7512), Oregon Green™ 488 BAPTA-1, AM, and Cell-permeant Special Packaging (No. O6807) were purchased from ThermoFisher Scientific (Shanghai, China). We also purchased an FITC Annexin V Apoptosis Detection Kit I (No. 556547) from BD Biosciences (Beijing, China). We also acquired a Minute™ Total Protein Extraction Kit (No. SD-001/SN-002) and a Mitochondria Isolation Kit For Mammalian Cells And Tissues (No. MP-007) from Invent (Beijing, China). We purchased a range of reagents from Cell Signaling Technology (Shanghai, China), including a PARP (46D11) Rabbit mAb (No. 9532), Caspase-3 (D3R6Y) Rabbit mAb (No. 14220), Cytochrome c (D18C7) Rabbit mAb (No. 11940), Smac/Diablo (D5S3R)

Rabbit mAb (No. 15108), Endonuclease G Antibody (No. 4969). We also purchased a monoclonal anti-ARTS antibody mAb (No. 106M4840) from Sigma-Aldrich (Shanghai, China). We purchased an anti-AIF antibody (No. ab1998), anti-HtrA2/Omi antibody (No. ab75982), anti-PERK antibody (No. ab65142), anti-ATF-6 (ab37149), anti-IRE1 (ab37073) from Abcam (Shanghai, China).

2.2 Methods

2.2.1 Annexin V analysis

HepG-2 cells were seeded at a density of 6×10^5 cells per well in a 6-well plate and incubated for 24 h at 37°C in 5% CO_2. Cells were then infected with Ad-Vp3 (MOI: 50) for 12, 24, 36, 48, and 72 h. Ad-Vp3-infected HepG-2 cells were incubated in the dark for 15 min at room temperature in the presence of 5 μL Annexin V-FITC and 5 μL of PI in 100 μL of 1 × binding buffer. We then quantified the extent of apoptosis in HepG-2 cells by flow cytometry. Ad-Mock-infected cells and non-infected HepG-2 cells were used as negative controls.

2.2.2 ROS levels analysis

HepG-2 cells were seeded at 6×10^6 cells per well in a 6-well plate and incubated for 24 h at 37°C with 5% CO_2. The cells were then infected with 50 MOI Ad-Vp3 for 12, 24, 36, 48, and 72 h. HepG-2 cells infected with Ad-Vp3 were incubated in the dark for 15 min at room temperature in the presence of 1 μL DHR in 1 mL of DMEM. Flow cytometry was used to detect the level of ROS in HepG-2 cells infected with Ad-Vp3. Ad-Mock-infected cells and non-infected HepG-2 cells were used as negative controls.

2.2.3 Electron microscopy

HepG-2 cells were seeded at a density of 6×10^5 cells/well into a 6-well plate, cultured for 24 h at 37°C in 5% CO_2, and infected with Ad-Vp3 (MOI: 50) for 48 h. Cells were then harvested, washed with PBS, and sections prepared using ultramicrotomy. Cells were analyzed by electron microscopy. Ad-Mock-infected cells and non-infected HepG-2 cells were used as negative controls.

2.2.4 Ca^{2+} levels analysis

HepG-2 cells were seeded at a density of 6×10^5 cells/well into a 6-well plate, cultured for 24 h at 37°C in 5% CO_2, and infected with Ad-Vp3 (MOI: 50) for 12, 24, 36, 48, and 72 h. Cells were then incubated in the dark for 20 min at 37°C, in the presence of 1 μg Oregon Green™ 488 BAPTA-1. We then quantified Ca^{2+} levels in the HepG-2 cells by fluorescence microscopy and flow cytometry, in accordance with the manufacturer's instructions. Ad-Mock-infected cells and non-infected HepG-2 cells were used as negative controls.

2.2.5 Mitochondrial analysis: structure and function

HepG-2 cells were seeded at a density of 6×10^5 cells/well into a 6-well plate, cultured for 24 h at 37°C in 5% CO_2 and infected with Ad-Vp3 (MOI: 50) for 12, 24, 36, 48, and 72 h. Cells were then incubated in the

dark for 20 min at 37°C in the presence of 1 μL JC-1 in 1 mL of DMEM. We then determined the mitochondrial membrane potential of HepG-2 cells by flow cytometry. Ad-Mock-infected cells and non-infected HepG-2 cells were used as negative controls.

For structural analysis, HepG-2 cells were seeded at a density of 1×10^7 cells into a 100 mm cell culture dish, cultured for 24 h at 37°C in 5% CO_2 and infected with Ad-Vp3 (MOI: 50) for 48 and 72 h. We then collected mitochondria by use of a Mitochondria Isolation Kit for Mammalian Cells and Tissues, in accordance with the manufacturer's guidelines. We then prepared sections by ultramicrotomy and investigated the structure of the mitochondria by electron microscopy Ad-Mock-infected cells and non-infected HepG-2 cells were used as negative controls.

2.2.6 Western blotting

HepG-2 cells were seeded at a density of 6×10^5 cells/well into a 6-well plate, cultured for 24 h at 37°C in 5% CO_2 and infected with Ad-Vp3 (MOI: 50) for 12, 24, 36, 48, and 72 h. Ad-Mock-infected cells were used as negative controls. Total protein was extracted from cells using the Minute™ Total Protein Extraction Kit, separated by SDS-PAGE, and transferred to membranes for Western blotting so that we could determine the expression levels of proteins related to apoptotic proteins, ER stress pathway and apoptotic pathways in the mitochondria.

2.2.7 Ca^{2+} imbalance analysis

HepG-2 cells were seeded at a density of 6×10^5 cells/well into a 6-well plate, cultured for 24 h at 37°C in 5% CO_2 and treated with Ad-Vp3 (MOI: 50) and 10 μM BAPTA-AM for 72 h. For Annexin V analysis, the cells were incubated in the dark for 15 min at room temperature in the presence of 5 μL Annexin V-FITC and 5 μL of PI in 100 μL of 1 × binding buffer. We then quantified the extent of apoptosis in HepG-2 cells by a fluorescence microscope and low cytometry. For Mitochondrial analysis, Cells were then incubated in the dark for 20 min at 37°C in the presence of 1 μL JC-1 in 1 mL of DMEM. We then determined the mitochondrial membrane potential of HepG-2 cells by a fluorescence microscope and low cytometry.

2.2.8 In vivo studies

The xenograft models were established via subcutaneous injection of HepG-2 cells (3×10^6/100 μL) with Matrigel® Matrix Basement Membrane (yielding a 1:1 ratio) into mice left legs. When the tumors had formed clearly (usually 14 days), the mice were divided randomly into five groups (9 mice per group). Group 1 was injected with 1×10^8 plaque forming units (PFU) of Ad-Vp3 and 5 mg/kg BAPTA-AM, group 2 was injected with Ad-Vp3 ($1x10^8$ PFU). Group 3 was injected with 5 mg/kg BAPTA-AM. Group 4 was injected with Ad-Mock (1×10^8 PFU) and group 5 was injected with the same volume of the vehicle. All groups were infected with Ad-Vp3 or Ad-Mock via intratumoral injection and treated with BAPTA-AM via intraperitoneal injection from the day 14. The injections were given every 3 days for 15 days. Tumor volumes (length × $width^2$ × 0.5) and survival rates were calculated every 7 days for 35 days. During the experiment, tumors from 3 mice and from each group were harvested. We then used Western-blot and

immunohistochemical staining to investigate the apoptotic pathway in the mitochondria, including AIF, HtrA2, Smac/Diablo, and Cyto-C. All immunohistochemical detection was performed by Servicebio (Wuhan, China). All animals' experimental procedures were approved by the Institutional Animal Care and Use Committee of the Changchun University of Chinese Medicine.

2.3 Statistics

All statistical analyses were performed by using the Statistical Package for the Social Sciences (SPSS) statistical software package (version 15.0; SPSS Inc., Chicago, IL, USA). Data were presented using GraphPad Prism version 7.0 (GraphPad Software Inc., La Jolla, CA, USA). For analysis, we used the Student's t-test or one-way analysis of variance (ANOVA) followed by Tukey's post-hoc test; $p < 0.05$, $p < 0.01$, or $P < 0.001$, were considered to be statistically significant. Data are presented as the mean ± standard deviation (SD).

Immunohistochemical analyses were performed using Image-Pro Plus 6.0 software (Media Cybernetics, Inc., Rockville, MD, USA). At least 3 fields of vision were randomly selected for each slice (and for each group). When acquiring images, we organized the entire field of view to ensure that the background illumination was consistent. The method was used to define positive staining in cells for other types of proteins; a brown/yellow stain indicated positive immunostaining. We used Image-Pro Plus 6.0 software to determine the integrated optical density (IOD) and the area occupied by the entire tissue (AREA). The Areal density was then defined by IOD/AREA. A larger areal density indicated a higher level of positive expression.

3 Results

3.1 Apoptosis of HepG-2 cell induced by Apoptin

The apoptosis of HepG-2 cell can be significantly induced by Apoptin (**Figure. 1A**). The apoptotic rate in Ad-Vp3-infected cells was significantly higher than that in Ad-Mock-infected cells and non-infected HepG-2 cells at 48 and 72 h post-infection ($p < 0.05$). The results of apoptosis-related proteins in Ad-Vp3-infected HepG-2 cells are shown in **Figure. 1B**. The expression levels of Cleaved-PARP and Cleaved-Caspase-3 in Ad-Vp3-infected HepG-2 cells were significantly higher at 48 and 72 h post-infection, when compared with HepG-2 cells infected with Ad-Mock ($p < 0.01$). The ROS levels of HepG-2 cells can be significantly induced by Apoptin (**Figure. 1C**). ROS levels in Ad-Vp3-infected cells were significantly higher than that in Ad-Mock-infected cells and HepG-2 cells at all time points ($p < 0.05$).

3.2 Apoptin induction of endoplasmic reticulum stress

Our analysis showed that some of the proteins related to ER stress pathway were significantly affected by Apoptin (**Figure. 2A and B**). For example, the expression of PERK and ATF-6 in Ad-Vp3-infected cells were significantly higher at 12 and 24 h than cells infected with Ad-Mock, but were significantly lower at 48 and 72 h post-infection ($p < 0.01$). The expression level of IRE1 in Ad-Vp3-infected cells was significantly higher than that in Ad-Mock-infected cells at all time points ($p < 0.01$).

The effect of Apoptin on the structure of the ER was evaluated by electron microscopy. Electron microscopy revealed clear structural damage in the ER and mitochondria of infected cells at 48 h (**Figure. 2C**). The structure of ER and the crest of the mitochondria in Ad-Vp3-infected cells had incurred significant damage by 48 h post-infection. This result indicated that the strong and lasting ER stress response can damage the structure of the ER.

The intensity of green fluorescence (as an indicator of Ca^{2+} level) in HepG-2 cells infected with Ad-Vp3 was significantly higher than cells infected with Ad-Mock at 24, 36, and 48 h, post-infection. At 72 h post-infection, the level of green fluorescence in the HepG-2 cells infected with Ad-Vp3 was significantly lower than that in the control group (**Figure. 2D and E**) ($p < 0.05$). The trend for green fluorescence over time was similar to that shown by flow cytometry (**Figure. 2F**). These results showed that ER stress increased the levels of Ca^{2+}, leading to an imbalance in Ca^{2+}. Therefore, Apoptin can induce a strong and lasting ER stress that ultimately leads to Ca^{2+} imbalance.

3.3 Effect of Apoptin on mitochondria

The mitochondrial membrane potential of HepG-2 cells was significantly reduced by Apoptin. The relative fluorescence (R2/R3; Red/Green) associated with mitochondrial membrane potential in Ad-Vp3-infected HepG-2 cells was significantly lower than that in Ad-Mock-infected cells and non-infected cells at 24, 36, 48 and 72 h post-infection (**Figure. 3A**) ($p < 0.05$).

It was also evident that Apoptin caused damage to the mitochondria of HepG-2 cells (**Figure. 3B**); the crest of the mitochondria in Ad-Vp3-infected cells appeared to be broken and dissolved at 48 h post-infection. At 72 h post-infection, it was evident that the mitochondria had been completely destroyed.

The expression levels of AIF, HtrA2, Smac/Diablo, and Cyto-C, in Ad-Vp3-infected cells were significantly higher than those in Ad-Mock-infected cells at all time points (**Figure. 3C and D**) ($p < 0.05$). However, there were no significant differences with regards to the expression of ARTs and Endo G in HepG-2 cells infected with Ad-Vp3 and Ad-Mock ($p > 0.05$). It was evident that Apoptin can trigger the apoptotic pathway in the mitochondria by increasing the expression levels of AIF, HtrA2, Smac/Diablo, and Cyto-C.

Collectively, these results indicated that Apoptin significantly reduced mitochondrial membrane potential, caused damage to the mitochondrial structure and triggered the apoptotic pathway in the mitochondria of HepG-2 cells.

3.4 BAPTA-AM reduced the apoptosis of HepG-2 cell induced by Apoptin

In order to verify whether Ca^{2+} imbalance has an effect in HepG-2 cells, we performed Annexin V and JC-1 analysis on Ad-Vp3-infected HepG-2 cells (Fig. 4A **and B**). The apoptotic rate in Ad-Vp3 + BAPTA-AM-treated cells and Ad-Vp3-infected cells was significantly higher than that in BAPTA-AM-treated cells, Ad-Mock-infected cells and HepG-2 cells, 72 h post-infection ($p < 0.001$), while that in Ad-Vp3 + BAPTA-AM-treated cells was significantly lower than that in Ad-Vp3-infected cells, 72 h post-infection (**Figure. 4A**) (p

< 0.01). The mitochondrial membrane potential of HepG-2 cells in Ad-Vp3 + BAPTA-AM group and Ad-Vp3 group was significantly higher than that in BAPTA-AM group, Ad-Mock group and HepG-2 group at 72 h post-infection ($p < 0.001$), while that in Ad-Vp3 + BAPTA-AM group was significantly higher than that in Ad-Vp3 group at 72 h post-infection (**Figure. 4B**) ($p < 0.01$). These results showed that apoptotic rate and mitochondrial membrane potential were significantly affected by Ca^{2+} imbalance.

3.5 Ca^{2+} level affected the antitumor ability of Apoptin in vivo

The antitumor effects of Ad-Vp3 can be significantly reduced by BAPTA-AM in the HepG2-xenografted nude mice. The tumor volume in the Ad-Vp3 + BAPTA-AM group was significantly lower than that in the Ad-Vp3 group, at 28 and 35 days after tumor xenografting (**Figure.5A and B**) ($p < 0.01$). The survival rate of the Ad-Vp3 group was 100%, while that of the Ad-Vp3 + BAPTA-AM group was 70%, 35 days after tumor xenografting, respectively. The survival rate in the Ad-Vp3 group was significantly longer than that in the Ad-Vp3 + BAPTA-AM group. (**Figure. 5C**) ($p < 0.01$). The KI67 positivity rate in the Ad-Vp3 + BAPTA-AM and Ad-Vp3 group tumors was significantly lower than that in the BAPTA-AM, Ad-Mock and PBS groups ($p < 0.0001$), while that in Ad-Vp3 + BAPTA-AM group was significantly higher than that in Ad-Vp3 group ($p < 0.01$). The Tunel positivity rate in the Ad-Vp3 + BAPTA-AM and Ad-Vp3 group tumors was significantly higher than that in the BAPTA-AM, Ad-Mock and PBS groups ($p < 0.0001$), while that in Ad-Vp3 + BAPTA-AM group was significantly lower than that in Ad-Vp3 group (**Figure. 5D**) ($p < 0.01$). These results showed that BAPTA-AM could significantly inhibit the antitumor effect of Apoptin.

3.6 Western-blot and immunohistochemical detection of mitochondrial apoptotic pathway related proteins in tumor tissues

Western-blot analysis of the tumor tissues showed that the expression levels of AIF, HtrA2, Smac/Diablo and Cyto-C in Ad-Vp3 + BAPTA-AM and Ad-Vp3 groups were significantly higher, when compared with BAPTA-AM, Ad-Mock and PBS groups ($p < 0.05$). While the expression levels of Smac/Diablo and Cyto-C in the Ad-Vp3 + BAPTA-AM group were significantly lower than that in the Ad-Vp3 group (**Figure. 6A**) ($p < 0.01$). The variation trend of expression levels of AIF, HtrA2, Smac/Diablo and Cyto-C in immunohistochemical data (**Figure. 6B**) was similar to that shown by Western-blot. Collectively, these *in vivo* results showed that Apoptin caused significant changes in the expression of AIF, HtrA2, Smac/Diablo and Cyto-C, while BAPTA-AM could reduce the expression of Smac/Diablo and Cyto-C in Apoptin-treated tumor tissues.

4. Discussion

The endoplasmic reticulum is a highly dynamic organelle that plays a key role in homeostasis. The homeostatic balance created by the ER can, however, be disrupted by genetic and environmental damage, thus resulting in ER stress. In order to restore dynamic balance, the ER stress pathway is triggered and

produces increased levels of several stress-related proteins, including PERK [2, 27, 28], IRE1 [4, 22], and ATF-6 [6, 10, 34]. Collectively, these proteins lighten the load on the ER by reducing misfolding and helping avoid the accumulation of unfolded proteins. In this study, we found that the expression levels of proteins in the ER stress pathway, including PERK and ATF-6, were significantly higher in the HepG-2 cells infected with Ad-Vp3 than cells infected with Ad-Mock when tested at 12 h and 24 h post-infection. These changes were caused by ER stress. However, the expression levels of these proteins in Ad-Vp3-infected cells were significantly lower than those in the Ad-Mock-infected cells, at 48 h and 72 h post-infection. These changes might be caused by ER stress injury. Electron microscopy also revealed that the ER in HepG-2 cells had incurred significant structural damage when assessed at 48 h post-infection. Collectively, these results indicated that the structure and function of the ER were both damaged by strong and persistent ER stress, thus resulting in the increased expression of ER-related proteins; subsequently, these ER-related proteins showed a significant decrease in expression. In conclusion, these data indicate that Apoptin can cause ER stress injury in HepG-2 cells by inducing strong and persistent ER stress.

From one perspective, ER stress and injury can both cause an increase in intracellular Ca^{2+} levels, thus resulting in Ca^{2+} imbalance [5, 8, 16]. The levels of Ca^{2+} in Ad-Vp3-infected cells were significantly higher than those in Ad-Mock-infected cells and non-infected HepG-2 cells at 24, 36, and 48 h post-infection. This result may have been caused by a strong and lasting ER stress, and consequential ER stress injury. However, the Ca^{2+} levels in the Ad-Vp3-infected cells were significantly lower than that in the control groups at 72 h post-infection. We believe that this result was due to the fact that the Ad-Vp3-infected cells underwent a significant extent of apoptosis. In the present study, Apoptin triggered the ER stress pathway in the ER, thus increasing the expression levels of PERK, IRE1 and ATF-6. Consequently, we believe that Apoptin can induce a strong and lasting ER stress and Ca^{2+} imbalance.

An imbalance in the intracellular concentration of Ca^{2+} can affect the mitochondrial membrane potential [18] and subsequently induce the release of pro-apoptotic proteins from the mitochondrial membrane mesenchyme [21]. Several pro-apoptotic proteins can be released from the mitochondria, including AIF, HtrA2, Endo G, ARTS, Smac/Diablo, and Cyto-C. AIF is a flavoprotein and represents the main protein responsible for Caspase-independent apoptosis. HtrA2 and Caspase are known to competitively bind Inhibitors of Apoptosis Proteins (IAP) [25, 26]. The interaction between these pro-apoptotic proteins and IAP can relieve the inhibition of caspase by IAP, thus allowing caspase to become activated and then induce apoptosis. Endo G is known to migrate to the nucleus and trigger cell apoptosis by causing DNA fragmentation [14, 29, 33]. ARTs are known to mediate various pro-apoptotic stimuli in order to induce apoptosis. The function of Smac/Diablo is the same as HtrA2 [23, 25]. In vitro, we found that the mitochondrial membrane potential of Ad-Vp3-infected cells was significantly lower than that in Ad-Mock-infected cells and non-infected HepG-2 cells at 24 post-infection. Furthermore, compared with all other timepoints, the mitochondrial membrane potential at 36 h post-infection, was also significantly reduced in the cells infected with Ad-Vp3. We speculate that this result might be caused by an abnormal change in intracellular Ca^{2+} level. In order to analyze whether Ca^{2+} imbalance affects the abnormal changes of mitochondrial membrane potential mediated by Apoptin in HepG-2 cells, Ad-Vp3 infected cells were

further treated with BAPTA-AM. These results showed that the imbalance of Ca^{2+} induced by Apoptin could reduce the mitochondrial membrane potential and induce the apoptosis. In vivo, the regulation of Ca^{2+} imbalance reduced the expression levels of Smac/Diablo and Cyto-C in Ad-Vp3 + BAPTA-AM group. This result showed that the Apoptin might increase the expression levels of Smac/Diablo and Cyto-C to inhibit the proliferation of HepG-2 cells in tumor bearing nude mice via inducing Ca^{2+} imbalance.

In this study, we found that Apoptin induced a strong and lasting ER stress and thus cause ER stress injury. These events subsequently led to an imbalance of intracellular Ca^{2+}, a reduction in mitochondrial membrane potential, a significant extent of damage in the mitochondrial structure, and an increase in the expression levels of Smac/Diablo, and Cyto-C, by triggering the mitochondrial apoptotic pathway in HepG-2 cells. However, it is not clear how Apoptin induces ER stress. We speculate that Apoptin-induced ER stress may be related to Apoptin-induced G2/M phase arrest [3, 13]. G2 phase involves the synthesis of a large number of RNAs and proteins. Therefore, G2/M phase arrest may cause an accumulation of unfolded or misfolding proteins, thus triggering the Unfolded Protein Response (UPR), thus leading to ER stress. Previous studies have not reported the specific relationship between G2/M phase arrest and UPR/ER stress. It is clearly evident that we now need to be able to elucidate the specific relationships between these three factors. By investigating the relationships between G2/M phase arrest, UPR, and ER stress, we may be able to enhance our understanding of the role of Apoptin-induced ER stress in Apoptin-induced apoptosis.

Declarations

DATA AVAILABILITY

All datasets generated or analyzed during this current study are included in this published article.

Author contributions

XYY, TXW, YL and YLZ conceived and performed the experiments and analysed the data. YQL, BB, JBF, JCH, SZL, ZRX, XY, ZRL, YRL, GZZ and NYJ conducted the mouse experiments. XL and CS overall supervised the experiments and revised the manuscript. All authors read and approved the final manuscript.

Acknowledgment

The authors would like to express their gratitude to EditSprings (https://www.editsprings.com/) for the expert linguistic services provided.

Funding

This study was sponsored by the Changchun Science and Technology Development Plan Project (NO. 21QC01) and the Science and Technology Research Planning Project of Jilin Provincial Department of

Education (NO. JJKH20220887KJ), and the National Natural Science Foundation of China (Grant no. 82151221).

Ethics approval and consent to participate The animal experiment protocols were approved by the Institutional Animal Care and Use Committee of the Changchun University of Chinese Medicine (Approval No. 2021078).

Informed consent Informed consent was obtained from all individual participants included in the study.

Consent for publication Not applicable.

Research involving human participants and/or animals The animal experimental protocols were approved by the IACUC of the Changchun Veterinary Research Institute, Chinese Academy of Agricultural Sciences (Changchun, China) (10ZDGG007). The manuscript does not contain human clinical studies or patient data.

Conflict of interests The authors declare that they have no competing interests.

References

1. Burek M, Maddika S, Burek CJ et al (2006) Apoptin-induced cell death is modulated by Bcl-2 family members and is Apaf-1 dependent. Oncogene 25:2213–2222. http://dx.doi.org/10.1038/sj.onc.1209258
2. Cao L, Xue M, Chen J et al (2020) Porcine parvovirus replication is suppressed by activation of the PERK signaling pathway and endoplasmic reticulum stress-mediated apoptosis. Virology 539:1–10. http://dx.doi.org/10.1016/j.virol.2019.09.012
3. Chaabane W, Ghavami S, Ma?Ecki A et al (2017) Human Gyrovirus-Apoptin Interferes with the Cell Cycle and Induces G2/M Arrest Prior to Apoptosis. Arch Immunol Ther Exp 65:545–552. http://dx.doi.org/10.1007/s00005-020-00570-w
4. Chakraborty R, Uddin S, Macoy DM et al (2020) Inositol-requiring enzyme 1 (IRE1) plays for AvrRpt2-triggered immunity and RIN4 cleavage in Arabidopsis under endoplasmic reticulum (ER) stress. Plant physiology and biochemistry. PPB 156:105–114. http://dx.doi.org/10.1016/j.plaphy.2020.09.002
5. Chanaday NL, Nosyreva E, Shin OH et al (2021) Presynaptic store-operated Ca(2+) entry drives excitatory spontaneous neurotransmission and augments endoplasmic reticulum stress. Neuron 109:1314–1332. e1315.http://dx.doi.org/10.1016/j.neuron.2021.02.023
6. Chen Z, Liu Y, Yang L et al (2020) MiR-149 attenuates endoplasmic reticulum stress-induced inflammation and apoptosis in nonalcoholic fatty liver disease by negatively targeting ATF6 pathway. Immunol Lett 222:40–48. http://dx.doi.org/10.1016/j.imlet.2020.03.003
7. Cheng X, Liu H, Jiang CC et al (2021) [Retracted] Connecting endoplasmic reticulum stress to autophagy through IRE1/JNK/beclin1 in breast cancer cells. Int J Mol Med 4810 3892/. ijmm.2021.4997http://dx.doi.org/10.3892/ijmm.2021.4997

8. Choi AY, Choi JH, Hwang KY et al (2021) Retraction Note to: Licochalcone A induces apoptosis through endoplasmic reticulum stress via a phospholipase Cgamma1-, Ca(2+)-, and reactive oxygen species-dependent pathway in HepG2 human hepatocellular carcinoma cells. Apoptosis: an international journal on programmed cell death. 10.1007/s10495-021-01698-6http://dx.doi.org/10.1007/s10495-013-0955-y
9. Choucair H, Rahman MK, Umashankar B et al (2021) The aryl-ureido fatty acid CTU activates endoplasmic reticulum stress and PERK/NOXA-mediated apoptosis in tumor cells by a dual mitochondrial-targeting mechanism. Cancer Lett 526:131–141. http://dx.doi.org/10.1016/j.canlet.2021.11.022
10. Clark EM, Nonarath HJT, Bostrom JR et al (2020) Establishment and validation of an endoplasmic reticulum stress reporter to monitor zebrafish ATF6 activity in development and disease. Dis Models Mech. 1310.1242/dmm.041426http://dx.doi.org/10.1242/dmm.041426
11. Danen-Van Oorschot AA, Van Der Eb AJ, Noteborn MH (2000) The chicken anemia virus-derived protein apoptin requires activation of caspases for induction of apoptosis in human tumor cells. J Virol 74:7072–7078. http://dx.doi.org/10.1128/jvi.74.15.7072-7078.2000
12. Jeurissen SH, Wagenaar F, Pol JM et al (1992) Chicken anemia virus causes apoptosis of thymocytes after in vivo infection and of cell lines after in vitro infection. J Virol 66:7383–7388. http://dx.doi.org/10.1128/JVI.66.12.7383-7388.1992
13. Jose GT, Destin WH, Albert EP et al (2004) The viral protein Apoptin associates with the anaphase-promoting complex to induce G2/M arrest and apoptosis in the absence of p53. Genes Dev 18:1952–1957. http://dx.doi.org/10.1101/gad.1198404
14. Li LY, Luo X, Wang X (2001) Endonuclease G is an apoptotic DNase when released from mitochondria. Nature 412:95–99. http://dx.doi.org/10.1080/15548627.2021.1874209
15. Liao X, Zhan W, Li R et al (2021) Irisin ameliorates endoplasmic reticulum stress and liver fibrosis through inhibiting PERK-mediated destabilization of HNRNPA1 in hepatic stellate cells. Biol Chem 402:703–715. http://dx.doi.org/10.1515/hsz-2020-0251
16. Lin H, Peng Y, Li J et al (2021) Reactive Oxygen Species Regulate Endoplasmic Reticulum Stress and ER-Mitochondrial Ca(2+) Crosstalk to Promote Programmed Necrosis of Rat Nucleus Pulposus Cells under Compression. Oxidative medicine and cellular longevity 2021:8810698. http://dx.doi.org/10.1155/2021/8810698
17. Liu Z, Zhu H, Ma Y et al (2021) AGEs exacerbates coronary microvascular dysfunction in NoCAD by activating endoplasmic reticulum stress-mediated PERK signaling pathway. Metab Clin Exp 117:154710. http://dx.doi.org/10.1016/j.metabol.2021.154710
18. Logue SE, Cleary P, Saveljeva S et al (2013) New directions in ER stress-induced cell death. Apoptosis 18:537–546. http://dx.doi.org/10.1007/s10495-013-0818-6
19. Maddika S, Booy EP, Johar D et al (2005) Cancer-specific toxicity of apoptin is independent of death receptors but involves the loss of mitochondrial membrane potential and the release of

mitochondrial cell-death mediators by a Nur77-dependent pathway. J Cell Sci 118:4485–4493. http://dx.doi.org/10.1242/jcs.02580

20. Maddika S, Mendoza FJ, Hauff K et al (2006) Cancer-selective therapy of the future: apoptin and its mechanism of action. Cancer Biol Ther 5:10–19. http://dx.doi.org/10.4161/cbt.5.1.2400
21. Maria H-H et al (2007) Control of Macroautophagy by Calcium, Calmodulin-Dependent Kinase Kinase-β, and Bcl-2. Mol Cell 26:193–205. http://dx.doi.org/10.1016/j.molcel.2006.12.009
22. Quan JH, Gao FF, Lee M et al (2020) Involvement of endoplasmic reticulum stress response and IRE1-mediated ASK1/JNK/Mcl-1 pathways in silver nanoparticle-induced apoptosis of human retinal pigment epithelial cells. Toxicology 442:152540. http://dx.doi.org/10.1016/j.tox.2020.152540
23. Saelens X, Festjens N, Walle LV et al (2004) Toxic proteins released from mitochondria in cell death. Oncogene 23:2861–2874. http://dx.doi.org/10.1038/sj.onc.1207523
24. Sircaik S, Roman E, Bapat P et al (2021) The protein kinase Ire1 impacts pathogenicity of Candida albicans by regulating homeostatic adaptation to endoplasmic reticulum stress. Cell Microbiol 23:e13307. http://dx.doi.org/10.1111/cmi.13307
25. Suzuki Y, Imai Y, Nakayama H et al (2001) A serine protease, HtrA2, is released from the mitochondria and interacts with XIAP, inducing cell death. Mol Cell 8:613–621. http://dx.doi.org/10.1016/s1097-2765(01)00341-0
26. Van Loo G, Van Gurp M, Depuydt B et al (2002) The serine protease Omi/HtrA2 is released from mitochondria during apoptosis. Omi interacts with caspase-inhibitor XIAP and induces enhanced caspase activity. Cell Death & Differentiation 9:20–26. http://dx.doi.org/10.1038/sj.cdd.4400970
27. Wang H, Dou S, Zhu J et al (2020) Ghrelin mitigates MPP(+)-induced cytotoxicity: Involvement of ERK1/2-mediated Nrf2/HO-1 and endoplasmic reticulum stress PERK signaling pathway. Peptides 133:170374. http://dx.doi.org/10.1016/j.peptides.2020.170374
28. Wang X, Han Y, Hu G et al (2020) Endoplasmic Reticulum Stress Induces miR-706, A Pro-Cell Death microRNA, in A Protein Kinase RNA-Like ER Kinase (PERK) and Activating Transcription Factor 4 (ATF4) Dependent Manner. Cell J 22:394–400. http://dx.doi.org/10.22074/cellj.2020.6873
29. Wang X, Zhuang Y, Fang Y et al (2021) Endoplasmic reticulum stress aggravates copper-induced apoptosis via the PERK/ATF4/CHOP signaling pathway in duck renal tubular epithelial cells. Environ Pollut 272:115981. http://dx.doi.org/10.1016/j.envpol.2020.115981
30. Yu Y, Wu D, Li Y et al (2021) Ketamine enhances autophagy and endoplasmic reticulum stress in rats and SV-HUC-1 cells via activating IRE1-TRAF2-ASK1-JNK pathway. Cell Cycle 20:1907–1922. http://dx.doi.org/10.1080/15384101.2021.1966199
31. Zhang HH, Li C, Ren JW et al (2021) OTUB1 facilitates bladder cancer progression by stabilizing ATF6 in response to endoplasmic reticulum stress. Cancer Sci 112:2199–2209. http://dx.doi.org/10.1111/cas.14876
32. Zhang Y, Jiang D, Jin Y et al (2021) Glycine Attenuates Citrobacter rodentium-Induced Colitis by Regulating ATF6-Mediated Endoplasmic Reticulum Stress in Mice. Mol Nutr Food Res 65:e2001065. http://dx.doi.org/10.1002/mnfr.202001065

33. Zhao T, Zhang H, Guo Y et al (2007) Granzyme K Directly Processes Bid to Release Cytochrome c and Endonuclease G Leading to Mitochondria-dependent Cell Death. J Biol Chem 282:12104–12111. http://dx.doi.org/10.1074/jbc.M611006200
34. Zhou X, Lu B, Fu D et al (2020) Huoxue Qianyang decoction ameliorates cardiac remodeling in obese spontaneously hypertensive rats in association with ATF6-CHOP endoplasmic reticulum stress signaling pathway regulation. Biomed pharmacotherapy = Biomedecine pharmacotherapie 121:109518. http://dx.doi.org/10.1016/j.biopha.2019.109518
35. Zhuang SM, Shvarts A, Van Ormondt H et al (1995) Apoptin, a protein derived from chicken anemia virus, induces p53-independent apoptosis in human osteosarcoma cells. Cancer Res 55:486–489. http://dx.doi.org/10.1007/BF01520296

Figures

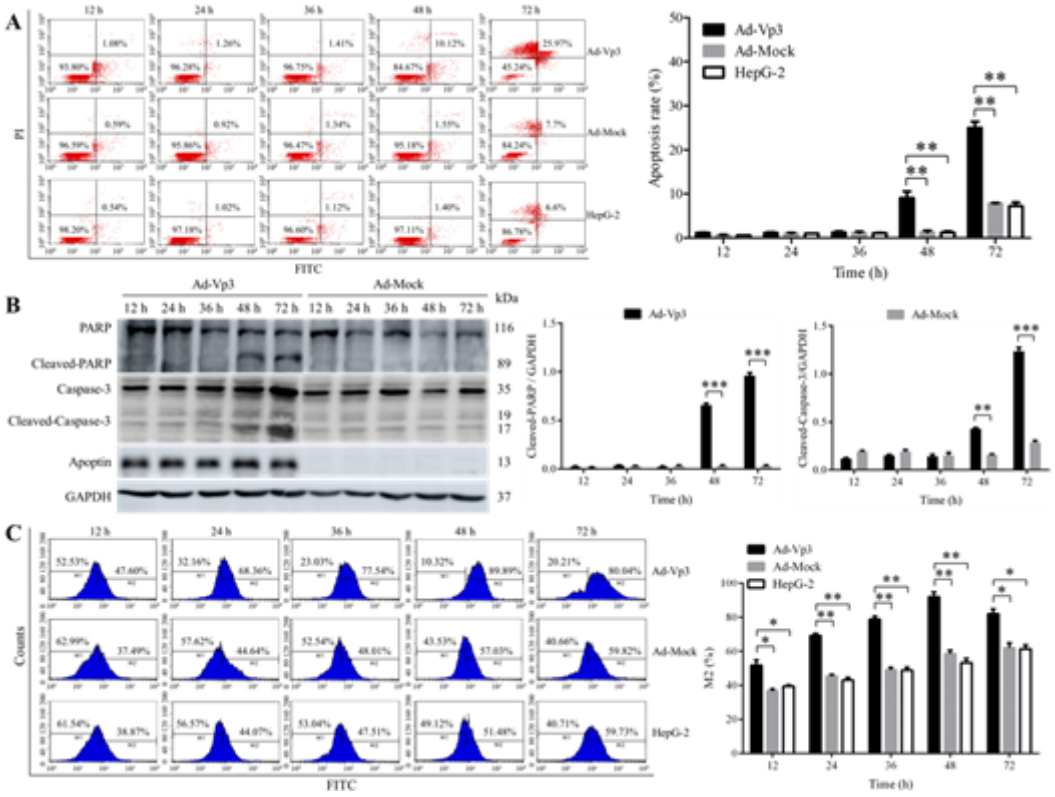

Figure 1

The apoptotic effects of Apoptin on HepG-2 cells. Apoptin significantly induced apoptosis in HepG-2 cells. **(A)** The detection of Annexin V-FITC/PI by flow cytometry in Ad-Vp3-infected HepG-2 cells. The apoptosis level of HepG-2 cells infected with Ad-Vp3 was significantly higher than that of other groups at 48 h and 72 h. **(B)** Western blot analysis of apoptosis-related proteins PARP and Caspase-3. The levels of Cleaved-PARP and Cleaved-caspase-3 in Ad-Vp3 group were higher than those in Ad-Mock at 48 h and 72 h. **(C)** The intracellular ROS was detected by flow cytometry. The level of ROS in Ad-Vp3 group were

significantly higher than that in Ad-Mock-infected cells and non-infected HepG-2 cells starting from 12 h to 72 h post-infection. Data are presented as mean ± SD, *p < 0.05, **p < 0.01, ***p < 0.001.

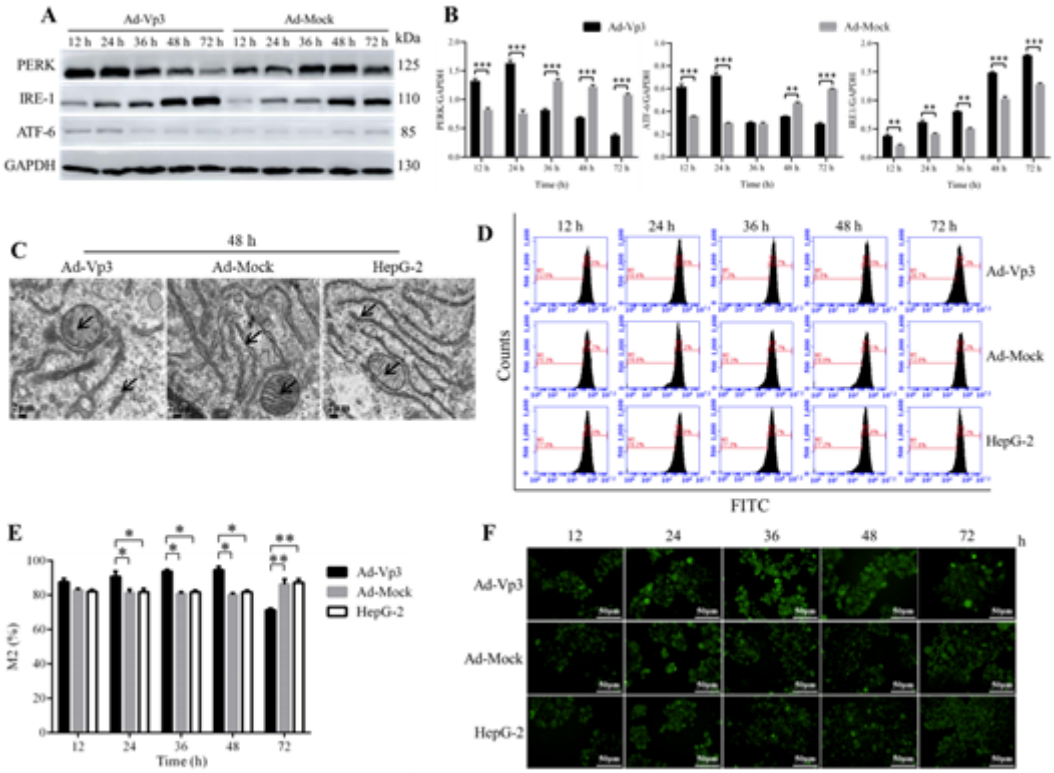

Figure 2

The effect of ER stress injury on HepG-2 cells. **(A, B)** Western blot analysis of the expression levels of proteins related to the ER stress pathway in ER. Apoptin triggered the ER stress pathway in the ER, which could increase the expression of PERK, IRE1 and ATF-6. **(C)** The structure of the ER in Ad-Vp3-infected HepG-2 cells was determined by electron microscopy at 48 h post-infection (5000×). The arrows represent ER and the mitochondria. The structure of the ER and the crest of the mitochondria in Ad-Vp3-infected cells had incurred damage at 48 h post-infection. The detection of Ca^{2+} levels and proteins related to the apoptotic pathway in the ER. Apoptin induces the imbalance of Ca^{2+} in HepG-2 cells infected with Ad-Vp3. **(D, E)** Flow cytometry detection of ER using Oregon Green™ 488 BAPTA-1, AM, cell permeant-Special Packaging. **(F)** Endoplasmic reticulum Oregon Green™ 488 BAPTA-1, AM, cell permeant-Special Packaging staining (200×). Data are presented as mean ± SD, *p < 0.05, **p < 0.01.

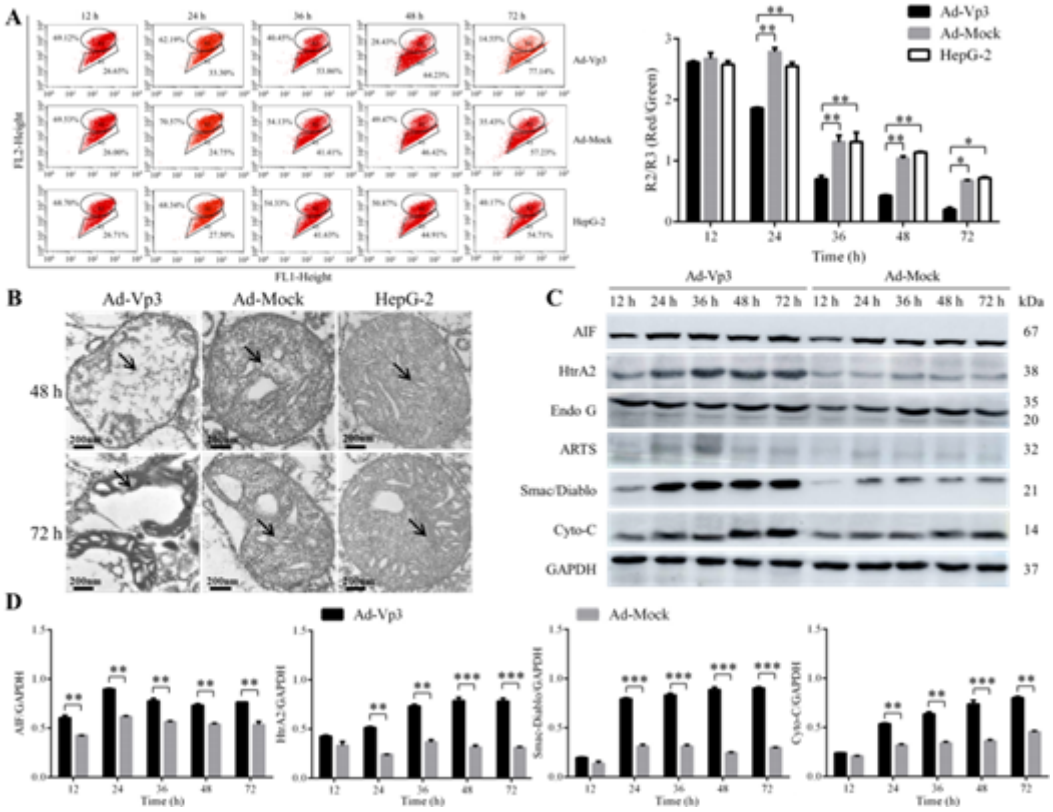

Figure 3

Apoptin significantly reduced mitochondrial membrane potential and caused damage to the mitochondrial structure. **(A)** Mitochondrial membrane potential, as determined by JC-1 and flow cytometry. **(B)** The structure of the mitochondria, as observed by electron microscopy at 48 and 72 h post-infection (30000×). The arrows represent mitochondria. The crest of the mitochondria in Ad-Vp3-infected cells had been broken and dissolved at 48 h post-infection. The mitochondria had been completely destroyed at 72 h post-infection. **(C, D)** Western blot analysis of the expression of proteins related to the apoptotic pathway in the mitochondria. Apoptin triggered the mitochondrial apoptotic pathway to increase the expression levels of AIF, HtrA2, Smac/Diablo, and Cyto-C. Data are presented as mean ± SD, *p < 0.05, **p < 0.01, ***p < 0.001.

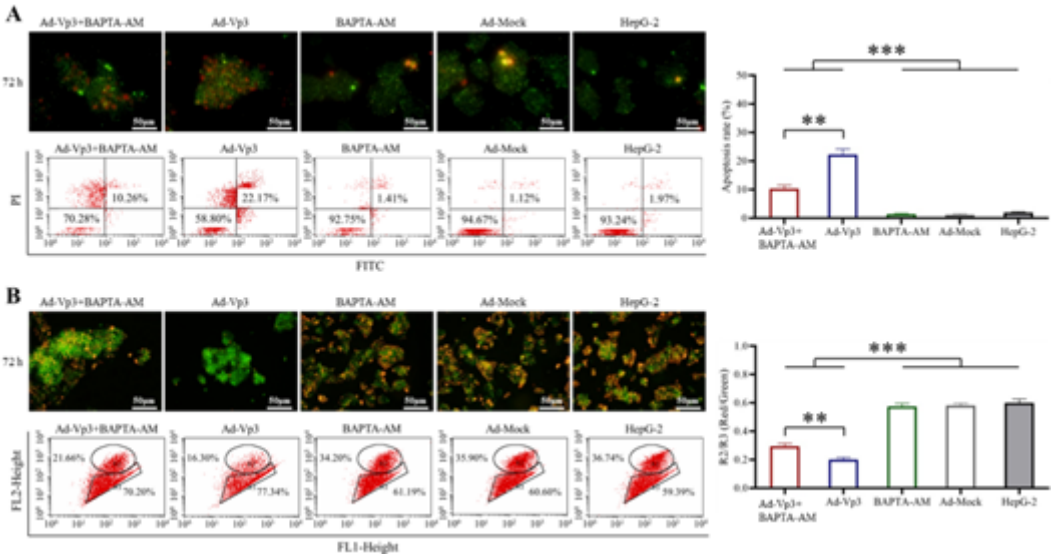

Figure 4

Relationship between Ca^{2+} level and apoptosis in HepG-2 cells infected with Ad-Vp3. **(A)** The detection of Annexin V-FITC/PI by flow cytometry and fluorescence staining at 72 h post-infection (200×). **(B)** Mitochondrial membrane potential, as determined by JC-1 flow cytometry and fluorescence staining at 72 h post-infection (200×). Data are presented as mean ± SD, **p < 0.01, ***p < 0.001.

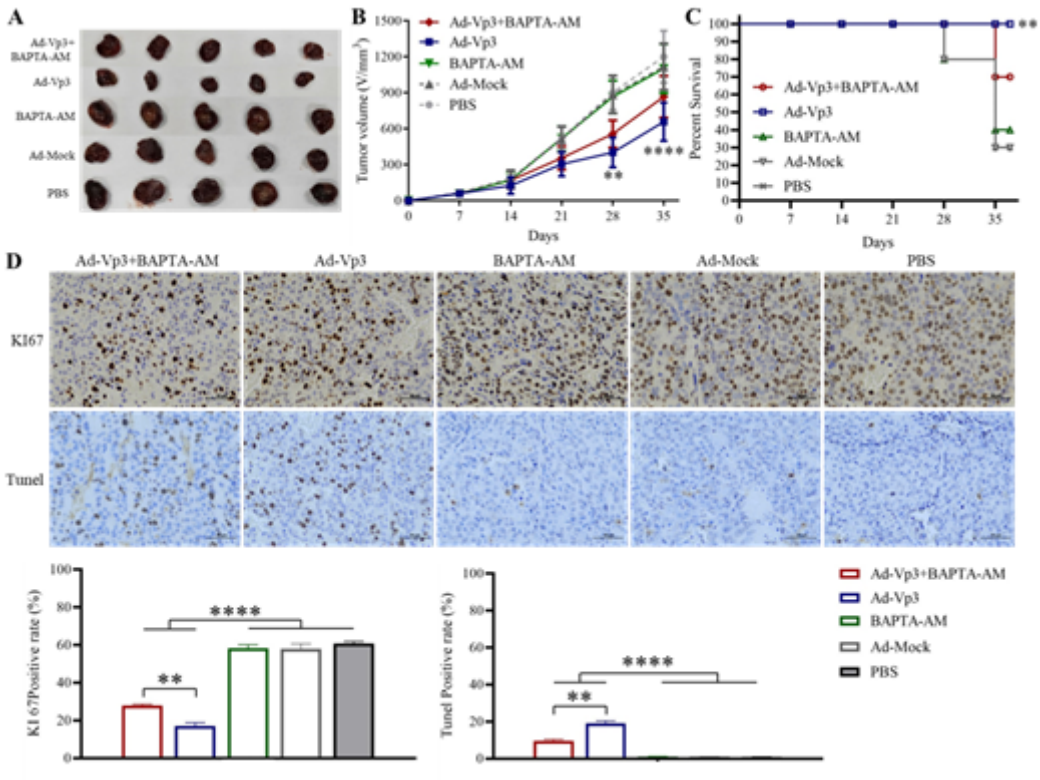

Figure 5

Inhibitory effect of Ad-Vp3+BAPTA-AM on HepG-2 cells in vivo. Apoptin significantly inhibits tumor growth and prolongs survival of tumor bearing nude mice, while BAPTA-AM significantly inhibited the antitumor effect of Apoptin. **(A, B)** The result of tumor growth inhibition. **(C)** The results of survival rate. **(D, E)** The results of immunocytochemistry detection of KI67 and Tunel in tumors' tissue (400×). Data are presented as mean ± SD, *p < 0.05, **p < 0.01.

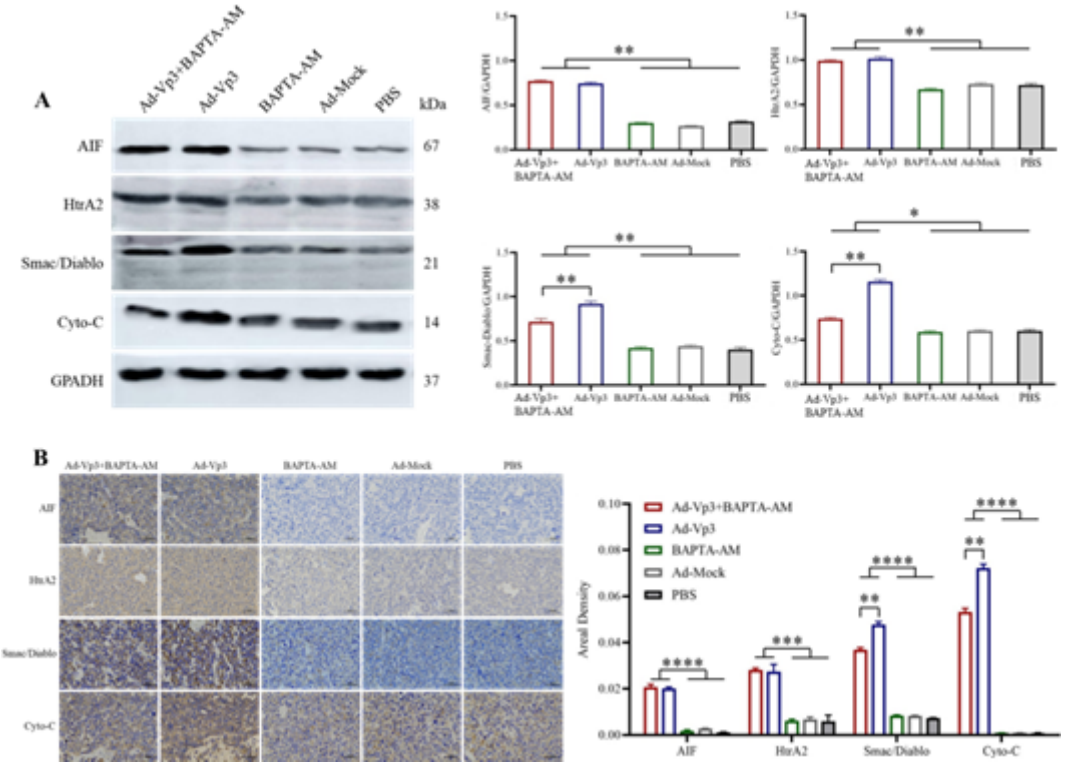

Figure 6

The Western-blot and immunohistochemical detection of apoptotic proteins related to the mitochondria. The expression of proteins related to apoptotic pathways in the mitochondria (AIF, HtrA2, Smac/Diablo, Cyto-C), as detected by Western-blot **(A)** and immunocytochemistry **(B)** (400×). Apoptin significantly induced the expression levels of AIF, HtrA2, Smac/Diablo, and Cyto-C, while BAPTA-AM significantly reduced the expression of Smac/Diablo and Cyto-C in Apoptin-treated tumor tissues. Data are presented as mean ± SD, *p < 0.05, **p < 0.01, ***p < 0.001, ****p < 0.0001.